Emruli, V. K., Liljedahl, L., Axelsson, U., Richter, C., Theorin, L., Bjartell, A., Lilja, H., Donovan , J., Neal, D., Hamdy, F. C., & Borrebaeck, C. A. K. (2021). Identification of a serum biomarker signature associated with metastatic prostate cancer. *Proteomics - Clinical applications*, *15*(2-3), [2000025]. https://doi.org/10.1002/prca.202000025

Received: 19 March 2020 | Revised: 10 January 2021 | Accepted: 11 January 2021 | Accepted article online: 13 February 2021

DOI: 10.1002/prca.202000025

Proteomics Clinical Applications

RESEARCH ARTICLE

Identification of a serum biomarker signature associated with metastatic prostate cancer

Venera Kuci Emruli[1] | Leena Liljedahl[1] | Ulrika Axelsson[1] | Corinna Richter[1] | Lisa Theorin[1] | Anders Bjartell[2,3] | Hans Lilja[3,4,5] | Jenny Donovan[6] | David Neal[5] | Freddie C. Hamdy[5] | Carl A. K. Borrebaeck[1]

[1] Department of Immunotechnology and CREATE Health Translational Cancer Center, Lund University, Lund, Sweden

[2] Department of Urology, Skåne University Hospital, Malmö, Sweden

[3] Department of Translational Medicine, Lund University, Malmö, Sweden

[4] Department of Laboratory Medicine, Surgery, and Medicine, Memorial Sloan Kettering Cancer Center, New York, New York, USA

[5] The Nuffield Department of Surgical Sciences, University of Oxford, Oxford, UK

[6] Bristol Medical School, University of Bristol, Bristol, UK

Correspondence
Professor Carl A. K. Borrebaeck, Department of Immunotechnology and CREATE Health, Lund University, Medicon Village, SE-22381 Lund, Sweden.
Email: carl.borrebaeck@immun.lth.se

Funding information
David H. Koch through the Prostate Cancer Foundation; National Institute for Health Research Oxford Biomedical Research Centre (Oxford NIHR BRC); Swedish Cancer Society, Grant/Award Number: CAN 2017/559; Vinnova, Grant/Award Number: UDI 2016-00462; Sidney Kimmel Center for Prostate and Urologic Cancers; UK National Institute for Health Research Health Technology Assessment Program, Grant/Award Numbers: projects 96/20/06, 96/20/99; CREATE Health Cancer Center; National Cancer Institute, Grant/Award Numbers: SPORE grant in Prostate Cancer [P50-CA92629], Support Grant to MSKCC [P30 CA008748]; Swedish Research Council, Grant/Award Number: (VR-MH project no. 2016-02974)

Abstract

Purpose: Improved early diagnosis and determination of aggressiveness of prostate cancer (PC) is important to select suitable treatment options and to decrease overtreatment. The conventional marker is total prostate specific antigen (PSA) levels in blood, but lacks specificity and ability to accurately discriminate indolent from aggressive disease.

Experimental design: In this study, we sought to identify a serum biomarker signature associated with metastatic PC. We measured 157 analytes in 363 serum samples from healthy subjects, patients with non-metastatic PC and patients with metastatic PC, using a recombinant antibody microarray.

Results: A signature consisting of 69 proteins differentiating metastatic PC patients from healthy controls was identified.

Conclusions and clinical relevance: The clinical value of this biomarker signature requires validation in larger independent patient cohorts before providing a new prospect for detection of metastatic PC.

KEYWORDS
affinity proteomics, antibody microarrays, biomarkers, cancer, prostate cancer

1 | INTRODUCTION

Prostate cancer (PC) is the fifth leading cause of cancer death among men worldwide and the second most commonly diagnosed cancer, with

Abbreviations: BE, backward elimination; HC, healthy controls; HC-1, healthy controls with total PSA ≤1 ng/mL; HC-2, healthy controls with total PSA > 1 ng/mL; IES, IMMray Evaluation Software; mPC, metastatic prostate cancer; mpMRI, multiparametric magnetic resonance imaging; nmPC, non-metastatic prostate cancer; PC, prostate cancer; PSA, prostate specific antigen; RRA, robust ranking algorithm; scFv, single-chain fragment variable; SVM, support vector machine

an estimated number of 1.3 million new cases in 2018 [1,2]. PC is a heterogeneous disease, exhibiting both indolent slow-growing tumors and more aggressive forms with rapid progression. The majority of PC patients are diagnosed with localized low or intermediate risk disease with a 5-year survival rate of nearly 100%, but a significant minority present with advanced or metastatic disease where the 5-year relative survival is only 30% [3,4]. Early and accurate determination of the disease state, particularly those with micro-metastases is crucial for selecting suitable therapeutic strategies to improve survival outcomes [5].

In current clinical practice, diagnosis of PC is made by digital rectal examination and measurement of total prostate specific antigen (PSA) levels in blood to decide if further investigations are necessary, such as imaging in the form of multiparametric magnetic resonance imaging (mpMRI) followed by transrectal or transperineal targeted/systematic ultrasound guided biopsies [6]. Despite the utility of PSA in triggering further tests, this marker lacks sufficient specificity as moderately elevated PSA levels appear also in non-malignant conditions, such as benign prostate hyperplasia and prostatitis. Consequently, many men without cancer or clinically insignificant PC undergo unnecessary investigations including biopsies with potential side effects, including life-threatening sepsis [7].

Intensive efforts have been made to find alternative diagnostic methods to stratify patients and improve early detection of clinically significant PC, such as PSA velocity, PSA density, proPSA isoforms, complexed PSA, and percentage of free PSA [8–11]. In addition, combinatorial approaches, such as prostate health index (PHI) and the four kallikrein panel (4Kscore), have been evaluated and shown improved accuracy at time of diagnosis and improved ability to discriminate Gleason≥7 [12,13]. Similarly, the Stockholm-3 (STHLM3) model and the later updated version, which is comprised of clinical variables, blood biomarkers, a genomic SNP panel and an explicit variable for the HOXB13 SNP, has displayed an improved prediction of Gleason ≥7 [14,15]. Furthermore, practice is changing rapidly in a large number of countries particularly in Europe whereby a pre-biopsy mpMRI is now triggered by an elevation in serum PSA, and guides targeted biopsies of the prostate; thus, reducing the over-detection of low-risk disease, and enhancing the diagnosis of intermediate and high-risk PC [16,17]. However, this continues to cause controversy, as targeted biopsies alone of visible lesions on mpMRI can miss up to 15% of important PC lesions [18–20].

In this study, we have focused on identifying blood-based biomarkers associated with metastatic PC disease at time of diagnosis, as this group of patients requires immediate intervention. We have used a high-throughput, recombinant antibody microarray targeting 157 analytes, mainly involved in immune regulation and cancer [21–25], to identify (i) serum proteins that discriminate patients with a metastatic prostate condition from healthy subjects; (ii) key pathways, and (iii) regulators, involved in metastatic PC disease.

Clinical Relevance

Prostate cancer (PC) is the second most commonly diagnosed cancer worldwide, and represents a heterogeneous disease, displaying both an indolent and aggressive behavior. Prognosis of PC is dependent on early and specific diagnosis of the disease. Prostate specific antigen (PSA) is a well-established diagnostic biomarker used in PC, but has limited specificity and ability to discriminate indolent from aggressive disease. Consequently, there is an urgent need for additional biomarkers that can add value to current diagnostic practices. In this study, we have shown that a number of low and high abundant proteins are elevated in serum derived from metastatic PC patients, compared to non-metastatic PC patients and/or healthy control patients. Importantly, we have identified a candidate serum biomarker signature that discriminates metastatic PC from healthy controls. Once validated in larger well-characterized clinical cohorts, these results might potentially provide a novel opportunity for the detection of metastatic PC, which requires immediate intervention.

2 | MATERIAL AND METHODS

2.1 | Clinical samples

In this retrospective study, 380 cryopreserved serum samples from the Oxford Biobank, consisting of serum from prostate cancer (PC) patients and healthy controls (HC) were assayed, out of which 363 samples were finally analyzed (Table 1). Samples were collected at different clinics in England from 2002–2014, centrifuged and serum was stored at −80°C. All prostate cancer samples, except one (discarded from analysis), were collected at time of diagnosis. Healthy controls (HC) were divided in two groups, (i) HC-1, including men with non-elevated total PSA (≤1 ng/mL) derived from the large ProtectT trial [26], and (ii) HC-2, including men with elevated total PSA (>1 ng/mL) and at least two negative biopsies. All samples were transported on dry ice to CREATE Health Translational Cancer Center at Lund University, Sweden, and upon arrival immediately stored at −80°C. Trial approval was obtained from the UK East Midlands (formerly Trent) Multicentre Research Ethics Committee (01/4/025), and informed consent was obtained from all participants.

2.2 | Biotinylation of serum samples

Sample IDs were recoded and all samples were randomized before biotinylation. Biotinylation steps were performed on ice or at 4°C

TABLE 1 Clinical samples included in the data analysis

	Healthy controls (HC)		Prostate cancer (PC)	
	HC-1	HC-2	nmPC	mPC
Number of samples	138	45	147	33
tPSA	0.7 (0.5–0.8)	8.1 (6.0–11.1)	6.7 (5.2–9.6)	270 (73.7–723.2)
Age	64 (62–68)	68 (63–72)	65 (62–71)	72 (64–82)
Digital rectal examination	NA	Normal	Normal or abnormal	Normal or abnormal
Total Gleason				
≤6			51 (34.9)	1 (2.9)
≥7			96 (65.3)	21 (63.6)
Unknown			0 (0)	11 (32.4)
T stage				
T1/T2			108 (73.5)	4 (12.1)
T3/T4			15 (10.3)	28 (82.4)
Unknown			24 (16.4)	1 (2.9)
M stage				
M0			31 (21.1)	0 (0)
M1			0 (0)	33 (100)[b]
Unknown			116 (78.9)[a]	0 (0)

All values are median (interquartile range) or frequency (%).
HC-1, healthy controls with total PSA ≤1 ng/mL; HC-2, healthy controls with total PSA >1 ng/mL; M stage, metastasis stage; mPC, metastatic prostate cancer; NA, not applicable; nmPC, non-metastatic prostate cancer; T stage, tumor stage; tPSA, total PSA (ng/mL).
[a]Cases with no indication or suspicion of metastatic disease at time of diagnosis.
[b]Indicated cases diagnosed with M1b.

in a Nunc™ 96-well polypropylene plate (Thermo Fisher Scientific, Waltham, USA). Briefly, crude serum samples were centrifuged at 16,000 x g, and 10 μL cleared serum was diluted in PBS (D-PBS-Sterile w/o Mg, Ca, GE Healthcare Life Sciences, Marlborough, USA) after which 2.56 mM Biotin (EZ-LinkTM NHS-PEG4-Biotin, Thermo Fisher Scientific) solution diluted in PBS (GE Healthcare Life Sciences) was added, to a final biotin concentration of 1.13 mM. The reaction was terminated after 2 h by adding 0.5 M Tris-HCl pH 8.0 (Thermo Fisher Scientific) to a final concentration of 181 mM. For each biotinylation plate, three replicates of a reference serum sample (ERM-DA470k/IFCC) [27] were included as process control. Biotinylated samples were aliquoted and stored at −80°C.

2.3 | Antibody production and purification

Human recombinant single-chain Fv (scFv) antibodies (n = 371, Table S1) directed against 158 proteins, mainly involved in immune regulation and cancer, were selected from in-house designed phage display scFv libraries [28,29]. ScFvs were purified from *E. coli* using His MultiTrap FF 96 well plates (GE Healthcare Life Sciences), according to manufacturer's protocol. Buffer exchange to PBS (GE Healthcare Life Sciences) was performed using Zeba™ 96-well desalt spin plates (Thermo Fisher Scientific), and thereafter 1% sodium azide (GBiosciences, Saint Louis, USA) was added to the purified scFv in PBS to a final concentration of 0.06%. The purity of the scFvs was evaluated by SDS-PAGE, using 8%—16% Criterion™ TGX Stain-Free™ Protein Gel (BioRad, Hercules, USA). The concentration was measured using a SPECTROstar Omega microplate reader and analyzed with the included MARS software (BMG Labtech, Ortenberg, Germany).

The specificity, affinity, and on-chip functionality of the scFvs has been assured using stringent phage display selection protocols [28,29], multiple clones (one to nine) per target, and a molecular design adapted for microarray application [30]. Moreover, the specificity of several of the antibodies has previously been validated using well-characterized human samples and orthogonal methods including ELISA, mass spectrometry, Meso Scale Discovery assay, cytometric bead assay and spiking and blocking experiments [25,29,31–37].

2.4 | Generation of antibody microarrays

Produced scFvs (concentration range 0.025–0.3 mg/mL) were printed (~330 pl/drop) on black polymer MaxiSorp slides (NUNC, Roskilde, Denmark), using a non-contact printer (SciFlexarrayer S11, Scienion, Berlin, Germany). Each scFv was printed in triplicate. PBS and Biotin-LC-BSA (Thermo Fisher Scientific) were included as negative and positive controls, respectively.

2.5 | Antibody microarray assay

Slides, consisting of multiple identical subarrays allowing up to seven different samples to be assayed on one single slide, were processed 6–9 days post microarray generation. A maximum of 15 slides were assayed at the same time. All samples were randomized over the different slides and assay days. In addition, on each array slide a quality control sample, denoted QCpool, consisting of pooled human serum from five healthy individuals, biotinylated at one occasion, was analyzed to allow evaluation of the inter-assay variability, meaning array-to array variations.

All incubation steps were performed at room temperature using a 3D rotator (PS-M3D, Progen Scientific, London, England) with reciprocal rotation (360°) for 9 s and vibration (5°) for 5 s. Briefly, slides were mounted in NEXTERION® IC-16 (Schott, Jena, Germany) multiwell incubation chambers, and blocked with MT-PBS (1% (w/v) nonfat dry milk (AppliChem GmbH, Darmstadt, Germany), 1% (v/v) Tween 20 (Merck KGaA, Darmstadt, Germany) in PBS) for 1 h. Arrays were washed four times with T-PBS (0.05% (v/v) Tween 20 in PBS) prior to incubation with diluted (1:50 in MT-PBS) biotinylated serum samples for 2 h. Next, slides were washed four times with T-PBS and then incubated with 1 μg/mL Alexa Fluor 647-Streptavidin (Thermo Fisher Scientific) for 1 h in darkness. Finally, slides were again washed four times with T-PBS, dismounted, quickly immersed in dH2O, and dried with compressed N_2 before scanning at 635 nm using the InnoScan 710AL with Mapix software (Innopsys, Carbonne, France).

2.6 | Data acquisition and pre-processing

The IMMray Evaluation Software (IES, Immunovia AB, Lund, Sweden) was used to align and quantify spot signal intensities. In total, 14 samples were not quantified due to poor quality images resulting from slide surface defects and/or uneven/high background. Additionally, one sample was removed due to other sampling time than at time of diagnosis. Using IES, local background was subtracted from each spot signal. Each data-point was represented by a mean spot intensity signal calculated based on three spot replicates per antibody. If the replicate coefficient of variation (CV) exceeded 15% from the mean value, the mean spot intensity was based on the two remaining replicates, which displayed most similar signals. At this stage, 7560 out of totally 135415 datapoints had a CV over 15%. Finally, all mean signals were trimmed, meaning that 5% of the lower and upper extreme values were discarded.

Quantified arrays were evaluated considering spot saturation, mean signal intensity, signal-to-noise ratio, and degree of missing points. Two samples (belonging to the HC-1 subgroup) were identified as outliers due to high degree of saturation over a large number of spots and were subsequently excluded. No antibodies were below the signal-to-noise ratio cutoff, defined as mean PBS signal $\pm$ 2 SD. In total, eight antibody clones targeting BIRC2, BTK, MCP-1, MUC1, ORP-3, PSA, PTN13, and TM-peptide had more than 5% missing values due to removal of spots with poor quality, and were consequently discarded from the final dataset, which consisted of 363 antibodies targeting 157 different proteins. Importantly, all eight targets except the TM-peptide, were still possible to measure using remaining clone(s) (one or several) targeting the same protein (Table S1). Remaining missing values (corresponding to 0.06% of all data-points) were replaced by bagged tree imputation [38]. Finally, acquired mean signal intensities were log2 transformed, visualized using 3D principal component analysis (PCA) (Qlucore AB, Lund, Sweden), and normalized using the Bayes algorithm ComBat [39] to adjust for batch (print-to-print) variation.

To assess the inter-assay variability, a total number of 173 QCpool samples were assayed. Of those, 37 samples were not quantified due to poor quality images resulting from slide surface defects and/or uneven/high background. The remaining 136 QCpool samples were quantified and used for calculation of the inter-assay CV. Briefly, CV values were first calculated per scFv for all slides within an assay day, then a mean CV value over 363 scFvs was calculated per assay day. The inter-assay CV was finally calculated as the average CV over 13 assay days. Importantly, the inter-assay CV was assessed for both raw data, and processed data (bagged tree imputed [38], log2 transformed and ComBat [39] normalized for print-to-print variation).

Raw and processed data is available through Figshare (https://doi.org/10.6084/m9.figshare.12370187).

2.7 | Data analysis

Sample and analyte distribution were assessed using PCA, and the performance of each analyte was evaluated using Wilcoxon rank sum test. Analytes with p-value $\leq$0.05 were considered as significantly different, either elevated or reduced in levels. Also, the Benjamini-Hochberg method was used for false discovery rate control. Moreover, for each analysis, selected sample groups were randomly divided into training and test set (70/30%), where the ratio of case versus control samples within the data sets was retained, and a backward elimination (BE) algorithm was applied using the training set, as previously described [40].

Briefly, using BE, proteins with the lowest discriminating contribution were eliminated, and analyte combinations with highest predictive power were identified. The signature length was selected based on the starting point where the lowest classification error occurred, and was used to build a support vector machine (SVM) classification model in the training set, which was then frozen and tested on the corresponding test set. The receiver operating characteristic (ROC) was used as error metric for all BE procedures and the area under curve (AUC) was used as a measure of the accuracy of performance of the signature in the test set. To minimize over-interpretation and to ensure robustness, a minimum of five independent BE procedures was performed, leading to a minimum of five signature lengths. Furthermore, each analyte in the different signatures was scored and ranked using a robust ranking algorithm (RRA) [41] based on the reverse order of elimination, where number one being the last analyte to be eliminated. To identify the signature with highest predictive classification accuracy, a consensus signature was generated by, (i) combining the results from the different

signatures, (ii) ranking the analytes based on a median RRA score, and (iii) eliminating analytes with an occurrence <60%.

Finally, to identify over-represented analytes and pathways, enrichment analysis (i.e., Enrichment analysis in Pathway Maps) was performed using MetaCore (Thomson Reuters, New York, NY, USA). A list consisting of all analytes targeted in the antibody microarray (Table S1) was set as background and used as reference for statistics in the enrichment analysis.

3 | RESULTS

3.1 | Assessment and handling of technical variation

A sample pool, QCpool, was used to analyze technical variation in the antibody microarray. Principle component analysis (PCA) of non-normalized (raw) log2 transformed QCpool data revealed print-to-print variations (Figure S1A). This variation was reduced using the Bayes algorithm ComBat [39], and confirmed by a PCA analysis of normalized data (Figure S1B). In addition, assessment of the inter-assay variation revealed a mean CV of 16% for non-normalized data, but only 2% after ComBat normalization (log2 transformed data), indicating further that the variation observed initially in the raw data could be handled by data processing.

Moreover, signals from binders targeting unique epitopes of the same analyte were compared with each other, and a median correlation coefficient of 0.8463 (including all possible comparisons, n = 336; interquartile range, 0.7049–0.9063) was observed. The variation is most probably due to differences in epitope specificity, as indicated by antibody sequence variances between clones targeting the same analyte.

3.2 | Analysis of discriminatory protein levels

In total, 363 clinical samples (Table 1) and 363 scFv, corresponding to 157 analytes were analyzed using Wilcoxon rank sum test. We identified 60 proteins that were elevated ($p \leq 0.05$) in samples from metastatic PC (mPC) patients compared to non-metastatic PC (nmPC) samples (Table 2). In addition, we identified 16 proteins to be elevated in mPC compared to samples from all healthy controls (HC). Fifteen of those 16 were also identified (by identical antibody clone) in the 60 analytes above, indicating an mPC-associated profile. These proteins were AMOT, Apo-A1, C5, CD40, CFAB, CYTC, DLG1, IL-6, IL-8, IL-16, JAK3, RANTES, STAP1, TNF-alpha and VEGFA, and their levels were all significantly higher in mPC compared to both nmPC and HC (data not shown). When comparing nmPC with HC, two proteins, C1q and UBC9, had significantly lower levels in nmPC (Table 2). Interestingly, UBC9 was also significantly lower in nmPC compared to mPC.

Using the recombinant antibody microarray, we did not observe any significant difference in PSA values between the different sample groups (HC, nmPC, mPC). However, these data demonstrated a lack of correlation to clinically measured PSA levels (Table 1), possibly due to dissimilarities in epitope specificities between the antibodies used in the two different assays.

3.3 | Identification of signatures for classification

To define a biomarker signature that classified mPC from healthy controls with non-elevated PSA (HC-1) we utilized BE-SVM, using five different training and test sets to test the model stability. This approach gave corresponding area under the curve (AUC) values in the test sets ranging from 0.68 to 0.81 (mean 0.74) (Figure 1). This variation depends on the limited number of samples included in the training sets, but still the data supports the fact that a discriminatory power exists in the different test sets classifying mPC from HC-1. Subsequently, the results were combined into a consensus signature consisting of 69 analytes targeted by 75 antibodies (Table 3). As expected, analytes from the consensus signature differed from those derived from the Wilcoxon test (Table 2), since different algorithms and sample groups (mPC vs. nmPC/HC in Wilcoxon test, and mPC vs. HC-1 in BE-SVM) were used. However, a total number of 27 analytes, including ATP-5B, C1 Inh, C4, C5, CCL11, CD40, CYTC, DLG2, DLG4, DPOLM, FAS, GNAI3, HCD2, HER2, IL-4, IL-16, IL-18, ITCH, MAPK1, MAPK8, MCP-1, NOS1, OSTP, PRDM8, PTN1, R-PTP-O and UBC9 were observed in both analyses, and were significantly upregulated in mPC compared to nmPC or HC, or both (Figure 2).

3.4 | Pathway analysis

To elucidate which pathways that are represented by the proteins found in the consensus signature discriminating mPC from HC-1 (Table 3), enrichment analysis using MetaCore (Thomson Reuters) was performed.

Among the significantly ($p \leq 0.05$) enriched pathway maps two PC associated pathways were defined, including (i) EGFR signaling in PC, and (ii) ligand-independent activation of androgen receptor in PC (Figure S2). Important top regulators in the identified pathway maps involve EGFR and ERBB2 (HER2), which together with downstream targets, promote cell proliferation and inhibition of apoptosis, supporting PC cell survival and growth (Figure S2).

Enrichment analysis was also performed for the analytes showing significant differential expression between mPC and nmPC (Table 2), and demonstrated significance considering regulation of angiogenesis in PC (Figure S3). Importantly, several proteins including among others TGF-beta-1, TNF-alpha, IL-1a and CCL2 (MCP-1) induce expression of VEGFA and IL-8, which are important regulators of angiogenesis and tumor neovascularization in PC (Figure S3).

Moreover, among the significantly enriched pathway maps, also immune response through the three complement pathways (classical, lectin and alternative pathway) was enhanced (data not shown), as levels of complement associated proteins including C1 Inh, C3, C4, C5 and CFAB were higher in mPC compared to nmPC (Table 2).

TABLE 2 Significantly ($p \leq 0.05$) differentially expressed analytes as derived from Wilcoxon rank sum test

mPC versus nmPC			mPC versus HC			nmPC versus HC		
Antibody	*p*-value	BH adj.[a] *p*-value	Antibody	*p*-value	BH adj.[a] *p*-value	Antibody	*p*-value	BH adj.[a] *p*-value
AMOT (2)	2.86E-02	6.75E-02	AMOT (2)	4.50E-02	6.75E-02	C1q	4.99E-02	1.07E-01
ANM5 (2)	2.62E-02	7.85E-02	Apo-A1 (1)	2.07E-02	6.21E-02	UBC9 (3)	3.28E-02	4.92E-02
Apo-A1 (1)	4.55E-02	6.82E-02	C5 (2)	1.20E-03	1.81E-03			
Apo-A4 (3)	3.14E-02	9.43E-02	CD40 (1)	4.51E-02	6.77E-02			
ATP-5B (1)	1.38E-02	4.14E-02	CFAB (3)	1.52E-02	2.27E-02			
C1 Inh (3)	4.73E-02	1.42E-01	CYTC (1)	1.78E-02	2.67E-02			
C3 (1)	3.69E-02	1.11E-01	DLG1 (2)	4.58E-02	6.87E-02			
C3 (5)	4.77E-02	1.43E-01	IL-16 (3)	3.18E-02	4.77E-02			
C4 (2)	2.85E-02	8.23E-02	IL-6 (2)	4.11E-02	6.16E-02			
C4 (3)	8.53E-03	2.56E-02	IL-6 (3)	3.95E-02	5.92E-02			
C4 (4)	3.57E-02	1.07E-01	IL-8 (1)	1.59E-02	2.67E-02			
C5 (2)	2.38E-04	7.14E-04	IL-8 (3)	1.77E-02	3.72E-02			
CCL11 (1)	2.48E-02	7.45E-02	JAK3	4.82E-02	7.22E-02			
CCL11 (2)	1.67E-02	5.00E-02	MCP-1 (8)	4.09E-02	1.23E-01			
CD40 (1)	1.71E-02	5.13E-02	RANTES (1)	3.93E-02	7.13E-02			
CFAB (1)	3.07E-02	9.21E-02	STAP1 (1)	3.36E-02	5.05E-02			
CFAB (3)	8.48E-03	2.27E-02	STAP1 (2)	4.90E-02	7.35E-02			
CYTC (1)	7.20E-03	2.16E-02	TNF-alpha (2)	4.82E-02	7.22E-02			
CYTC (4)	3.98E-02	1.04E-01	VEGFA (3)	2.35E-02	3.53E-02			
DLG1 (2)	2.80E-02	6.87E-02						
DLG2 (1)	4.82E-02	1.44E-01						
DLG2 (2)	3.72E-02	1.12E-01						
DLG4 (1)	4.65E-02	1.40E-01						
DPOLM (2)	3.66E-02	1.10E-01						
FAS (2)	4.63E-02	1.39E-01						
FER (2)	4.88E-02	1.46E-01						
GNAI3 (2)	3.20E-02	9.61E-02						
HCD2 (1)	3.56E-02	1.01E-01						
HCD2 (4)	4.47E-02	1.34E-01						
HER2 (2)	3.16E-02	9.47E-02						
HsMAD2 (2)	3.29E-02	9.87E-02						
IFN-gamma (2)	4.51E-02	1.35E-01						
IL-12 (1)	2.96E-02	7.78E-02						
IL-16 (3)	2.36E-02	4.77E-02						
IL-18 (1)	4.06E-02	1.15E-01						
IL-1a (1)	4.67E-02	1.40E-01						
IL-1a (3)	2.06E-02	6.17E-02						
IL-2 (1)	3.54E-02	8.09E-02						
IL-4 (1)	1.10E-02	3.31E-02						
IL-6 (2)	1.78E-02	5.34E-02						
IL-6 (3)	2.60E-02	5.92E-02						
IL-6 (5)	3.06E-02	9.17E-02						

(Continues)

TABLE 2 (Continued)

mPC versus nmPC			mPC versus HC			nmPC versus HC		
Antibody	*p*-value	BH adj.[a] *p*-value	Antibody	*p*-value	BH adj.[a] *p*-value	Antibody	*p*-value	BH adj.[a] *p*-value
IL-8 (1)	1.78E-02	2.67E-02						
IL-8 (3)	2.48E-02	3.72E-02						
IL-9 (3)	4.73E-02	9.22E-02						
ITCH (1)	3.61E-02	1.08E-01						
JAK3	4.55E-02	7.22E-02						
KCC2B (1)	3.25E-02	9.74E-02						
KCC2B (2)	4.22E-02	1.09E-01						
MAPK1 (2)	2.48E-02	7.45E-02						
MAPK8 (1)	4.06E-02	1.14E-01						
MARK2 (1)	3.20E-02	9.61E-02						
MCP-1 (6)/CCL2 (6)	1.25E-02	3.75E-02						
MUC1 (5)	2.93E-02	8.79E-02						
MYOM2 (2)	4.49E-02	1.17E-01						
NOS1 (2)	2.63E-02	7.89E-02						
OSTP (1)	3.69E-02	1.11E-01						
P85A (3)	3.69E-02	1.11E-01						
PGAM5 (1)	4.84E-02	1.45E-01						
PRDM8 (1)	3.23E-02	9.69E-02						
PRDM8 (2)	3.19E-02	9.56E-02						
PTK6	3.86E-02	1.16E-01						
PTN1 (1)	2.65E-02	7.96E-02						
RANTES (1)	4.75E-02	7.13E-02						
RANTES (3)	4.43E-02	9.25E-02						
R-PTP-kappa (2)	4.84E-02	1.45E-01						
R-PTP-O (1)	2.12E-02	6.35E-02						
STAP1 (1)	1.53E-02	4.59E-02						
STAP1 (2)	1.76E-02	5.29E-02						
STAT1 (2)	3.83E-02	1.15E-01						
TGF-beta-1 (1)	4.75E-02	1.43E-01						
TNF-alpha (2)	2.57E-02	7.22E-02						
UBC9 (3)	3.16E-03	9.47E-03						
UBE2C (2)	4.37E-02	1.31E-01						
UCHL5	3.61E-02	1.08E-01						
VEGFA (3)	1.90E-02	3.53E-02						

Raw *p*-values were adjusted using the Benjamini-Hochberg method. For analytes targeted by multiple clones, the individual antibody clone suffix is shown within brackets.

HC, healthy controls; mPC, metastatic prostate cancer; nmPC, non-metastatic prostate cancer.

[a]BH adj., Benjamini-Hochberg adjusted.

4 | DISCUSSION

Identification of metastases in PC patients has a major impact on treatment selection and overall survival outcome [42]. In spite of novel emerging imaging techniques showing improved ability to detect clinically significant PC [17] and metastatic PC (mPC) [43], there are still limitations considering the diagnostic accuracy including the dependence on an experienced radiologist interpretation [44]. As of today,

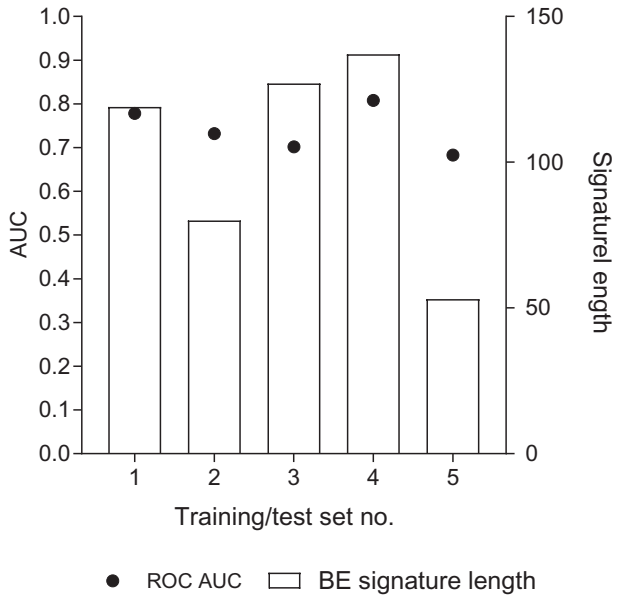

FIGURE 1 Backward elimination and support vector machine (BE-SVM) based classification of metastatic prostate cancer (mPC) versus healthy controls with total PSA ≤1 ng/mL (HC-1). Signature lengths generated from five different BE iterations, and corresponding AUC values from SVM model evaluation on the test sets

there is a lack of alternative non-invasive methods that could discriminate mPC with sufficient sensitivity and specificity at time of diagnosis.

In the present study we used an antibody-based microarray to identify a consensus biomarker signature that discriminate mPC from healthy controls with non-elevated PSA (HC-1). Due to the limited number of samples from metastatic patients the outcome of the analysis and the biomarker signature indicated model instability. To circumvent and improve this and to finally identify a signature with clinical utility, several development steps are needed. First, patient cohorts with similar diagnosis collected from different hospitals need to be tested to estimate the individual contribution of each biomarker to the performance of the signature. Secondly, this will allow us to reduce and refine the signature to minimize potential false positive analytes. Finally, the resulting biomarker signature should be evaluated with blinded samples in a multicenter program to be able to deliver clinical utility.

Nevertheless, using part of our data as a training set, we employed backward elimination and a supervised learning model (SVM) for reduction and classification purpose, and identified a consensus biomarker signature consisting of 69 analytes, which demonstrated the possibility to discriminate mPC from HC-1. In parallel, we applied a non-parametric statistical test (Wilcoxon rank sum test) to the entire set of mPC and non-metastatic PC (nmPC) samples, to identify significantly altered analytes. This analysis revealed 60 analytes as elevated in mPC compared to nmPC, where 27 of the 60 analytes overlapped with the consensus signature. The two different bioinformatic strategies gave, as expected, somewhat different outcome due to variations between the control groups (HC-1 in BE-SVM vs. nmPC in Wilcoxon rank sum test), as well as in the utilized algorithms (BE-SVM

TABLE 3 Consensus signature of analytes classifying samples as mPC or HC-1

mPC versus HC-1	Occurrence (%) in total no. of signatures	Median RRA[a] score
CYTC (1)	100	4
IgM (2)	100	8
C5 (2)	100	9
MCP-1 (9)	100	36
PTPRD (2)	100	45
MAPKK 2 (1)/MEK2 (1)	100	56
GLP-1R	80	10
Lewis y	80	15
HER2 (1)/ERBB2 (1)	80	19.5
MATK (3)	80	20.5
GNAI3 (2)	80	26
IL-16 (3)	80	29
OSTP (3)	80	29
HCD2 (2)	80	32.5
PRD14 (1)	80	39.5
ITCH (1)	80	41
HCD2 (3)	80	42
KSYK (1)	80	42.5
OSTP (2)	80	44.5
KKCC1 (1)	80	48
C4 (2)	80	49
OTUB2 (2)	80	49
PRD14 (2)	80	59.5
ATP-5B (2)	80	64.5
IL-18 (2)	80	66.5
SHC1 (2)/Shc (2)	80	77.5
UBC9 (1)	80	82
GLP-1	60	8
C1 Inh (4)	60	10
SOX11	60	10
PROP	60	12
HLA-DR/DP	60	15
NOS1 (1)	60	16
CCL11 (2)	60	18
GM-CSF (4)	60	20
C1 Inh (2)	60	22
KGP2 (1)	60	24
MAPK1 (3)/Erk1/2 (3)	60	26
CKIe (2)	60	27
PTN1 (3)	60	30
DLG4 (1)	60	30
GAK (3)	60	31

(Continues)

TABLE 3 (Continued)

mPC versus HC-1	Occurrence (%) in total no. of signatures	Median RRA[a] score
R-PTP-T (2)	60	32
MAPK8 (3)	60	34
EGFR	60	36
MCP-3 (1)	60	39
OTUB1 (1)	60	39
IL-4 (2)	60	41
APLF (2)	60	43
KCC4 (1)	60	44
PTPR2 (2)	60	45
PTPRD (1)	60	46
KRAS	60	48
R-PTP-O (1)	60	51
TNR14 (1)	60	54
FAS (4)	60	55
TENS4	60	55
MAPKK 6 (2)	60	55
PAR-6B (1)	60	58
CD40 (3)	60	58
IL-10 (1)	60	61
HsHec1 (2)	60	62
DLG2 (1)	60	62
IL-1ra (3)	60	69
ARHGC (1)	60	69
OTU6B (2)	60	74
PARP-1	60	75
BIRC2 (1)	60	77
PRDM8 (2)	60	78
PKB gamma (1)/AKT (1)	60	79
MCP-4 (1)	60	83
TNF-beta (4)	60	84
DPOLM (1)	60	86
MATK (1)	60	98
TNR3 (3)	60	99

The analytes in the consensus signature are based on the occurrence in five backward elimination iterations, sorted by highest combined score. For analytes targeted by multiple antibody clones, the individual antibody clone suffix is shown within brackets.

HC-1, healthy controls with total PSA ≤1 ng/mL; mPC, metastatic prostate cancer.

[a]RRA = robust ranking algorithm.

vs. Wilcoxon rank sum test). We believe that this comparative approach is crucial to circumvent any biases and limitations related to the use of one single method, in particular in absence of an independent validation cohort. Moreover, to further understand the biological context of the obtained results we performed enrichment analysis, which allowed us to identify enriched pathways in our datasets. This could also elucidate which of the identified proteins in the consensus biomarker signature and among the 60 analytes elevated in mPC versus nmPC, were enriched in PC associated pathways and are key findings with respect to mPC. Based on enrichment analysis in pathways, as a holistic approach to combine the results derived from BE-SVM and the Wilcoxon rank sum test, we identified EGFR, ERBB2 (HER2), IL-8 and VEGFA as potential important regulators of mPC. Noteworthy, despite the fact that only HER2 being a common denominator between the two bioinformatic approaches (BE-SVM and Wilcoxon rank sum test), we believe that the biological relevance of EGFR, IL-8 and VEGFA may be equally important in the context of mPC, which is also supported by previous findings reported in the literature, as discussed below.

Both EGFR and ERBB2 are members of the ERBB family of signaling receptors. Recent finding shows that ERBB2 and EGFR overexpression on a cellular level support metastatic progression of PC to bone [45]. In addition, higher expression of EGFR has been observed in exosomes derived from PC serum compared to healthy subjects [46], and serum levels of ERBB2 have been correlated with presence of metastatic prostate disease [47]. In line with these observations, we found upregulation of ERBB2 in mPC compared to nmPC, and presence of ERBB2 and EGFR in the consensus biomarker signature discriminating mPC from HC-1. Of note, high serum EBBR2 and EGFR levels have also been associated with advanced stage of breast cancer [48] and malignant pleural mesothelioma [49], respectively, potentially indicating a common role in disease progression, not necessarily limited to PC.

We also observed IL-8 to be significantly upregulated in mPC compared to both nmPC and HC. In consistency with our results, a significant elevation of IL-8 has been observed in men with PC bone metastases, compared to men with localized PC disease [50]. In addition, recent findings demonstrate that IL-8 is associated with PC aggressiveness and androgen receptor loss in primary and metastatic PC disease [51]. Importantly, expression of IL-8 has also been shown to correlate with PC tumorigenicity, metastasis and angiogenesis [52,53]. Likewise, also VEGFA plays a critical role in promoting angiogenesis in PC, leading to enhanced formation of blood vessels and further support of tumor growth [54], which likely contributes to tumor spread and development of metastasis. In this context, stimulation of VEGFA from prostate tumor cells has been demonstrated to be specifically mediated through binding of the cytokine CCL2 to its receptor on PC cells [54]. Importantly, also elevated plasma levels of VEGFA have been reported in metastatic PC compared with localized PC or healthy controls [55]. In agreement with these findings, we observed upregulation of VEGFA and CCL2 in mPC compared to both nmPC and HC, further emphasizing their involvement in metastatic PC disease.

Together, our findings suggest that EGFR, ERBB2, IL-8 and VEGFA are potential important regulators involved in metastatic PC disease. Also, additional analytes, including among others different cytokines (IL-1a, IL-2, IL-4, IL-6, IL-9, IL-12, IL-16, IL-18, RANTES), complement proteins (CFAB, C3, C4, C5) and apolipoproteins (Apo-A1, Apo-A4) were observed to be elevated in mPC compared to nmPC. Some

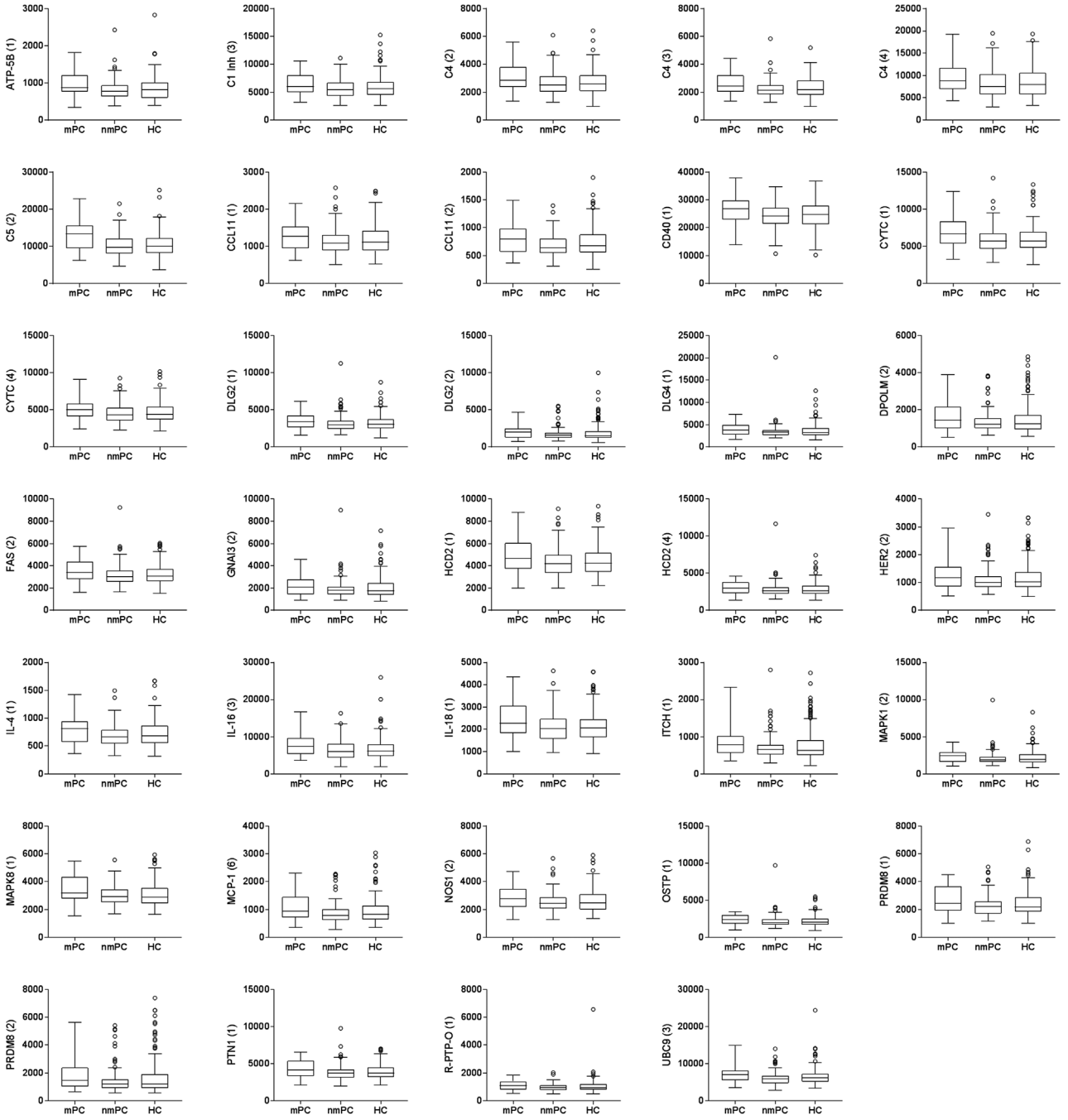

FIGURE 2 Significantly ($p \leq 0.05$, Wilcoxon rank sum test) elevated analytes in metastatic prostate cancer (mPC) compared to non-metastatic prostate cancer (nmPC) and/or healthy controls (HC) overlapping (either by identical or non-identical antibody clone(s)) with the consensus signature

of them have been related to PC aggressiveness (IL-4) [56], progressiveness (IL-6, IL-16),[57–59] invasion (RANTES) [60], metastases (IL-8) [61,62], and transition of androgen-dependent to androgen-independent phenotype (IL-6) [63], while others have not; thus, opens up for further research of their association to PC.

In summary, we have identified the first biomarker signature that discriminates mPC at diagnosis from HC-1. Furthermore, we also identified both low and high abundant proteins as elevated in serum derived from mPC compared to nmPC and/or HC. These findings indicate that our antibody-based microarray platform can be used to retrieve information on the systemic response of prostate cancer. To translate the identified biomarker signature into clinical utility additional studies are needed, as described. Furthermore, cohort sizes and inclusion of additional control samples from asymptomatic patients should be carefully designed to obtain clinical actionable information with an acceptable statistical power. Nevertheless, our findings presented herein represent a first step in paving the way towards a clinically useful biomarker signature associated with metastatic prostate cancer.

ACKNOWLEDGMENTS

This study was supported by funding from Vinnova (UDI 2016-00462) and CREATE Health Cancer Center at Lund University. Hans Lilja was supported in part by the National Institutes of Health/National Cancer Institute (NIH/NCI) with a Cancer Center Support Grant to Memorial Sloan Kettering Cancer Center (MSKCC) [P30 CA008748], a SPORE grant in Prostate Cancer [P50-CA92629], the Sidney Kimmel Center for Prostate and Urologic Cancers, David H. Koch through the Prostate Cancer Foundation, the Swedish Cancer Society (CAN 2017/559), and the Swedish Research Council (VR-MH project no. 2016–02974). The ProtecT trial is funded by the UK National Institute for Health Research Health Technology Assessment Program (projects 96/20/06, 96/20/99, http://www.nets.nihr.ac.uk/projects/hta/962099) with the University of Oxford as sponsor. Department of Health disclaimer: The views and opinions expressed therein are those of the authors and do not necessarily reflect those of the Department of Health. Freddie Hamdy is supported in part by the National Institute for Health Research Oxford Biomedical Research Centre (Oxford NIHR BRC).

CONFLICT OF INTEREST

Hans Lilja holds a patent on assays to measure intact PSA and is named on a patent for a statistical method to detect prostate cancer that has been commercialized as 4Kscore test by OPKO Health. Hans Lilja receives royalties from sales of the test and has stock in OPKO Health.

DATA AVAILABILTIY STATEMENT

The raw and processed data from this study are deposited in the Figshare repository, https://doi.org/10.6084/m9.figshare.12370187.

ORCID

Venera Kuci Emruli https://orcid.org/0000-0002-9527-0809

REFERENCES

1. Bray, F., Ferlay, J., Soerjomataram, I., Siegel, R. L., Torre, L. A., & Jemal, A. (2018). Global cancer statistics 2018: GLOBOCAN estimates of incidence and mortality worldwide for 36 cancers in 185 countries. *CA: A Cancer Journal for Clinicians*, *68*, 394–424.
2. Filippou, P., Ferguson, J. E. 3rd, & Nielsen, M. E. (2016). Epidemiology of prostate and testicular cancer. *Seminars in Interventional Radiology*, *33*, 182–185.
3. N. C. Institute, National Cancer Institute (2018).
4. Siegel, R. L., Miller, K. D., & Jemal, A. (2015). Cancer statistics, 2015. *CA: A Cancer Journal for Clinicians*, *65*, 5–29.
5. Johansson, J. E., Andren, O., Andersson, S. O., Dickman, P. W., Holmberg, L., Magnuson, A., & Adami, H. O. (2004). Natural history of early, localized prostate cancer. *JAMA*, *291*, 2713–2719.
6. Heidenreich, A., Bastian, P. J., Bellmunt, J., Bolla, M., Joniau, S., van der Kwast, T., Mason, M., Matveev, V., Wiegel, T., Zattoni, F., & Mottet, N. (2014). EAU guidelines on prostate cancer. part 1: Screening, diagnosis, and local treatment with curative intent-update 2013. *European Urology*, *65*, 124–137.
7. Loeb, S., Vellekoop, A., Ahmed, H. U., Catto, J., Emberton, M., Nam, R., Rosario, D. J., Scattoni, V., & Lotan, Y. (2013). Systematic review of complications of prostate biopsy. *European Urology*, *64*, 876–892.
8. Brawer, M. K., Aramburu, E. A., Chen, G. L., Preston, S. D., & Ellis, W. J. (1993). The inability of prostate specific antigen index to enhance the predictive the value of prostate specific antigen in the diagnosis of prostatic carcinoma. *The Journal of Urology*, *150*, 369–373.
9. Lein, M., Semjonow, A., Graefen, M., Kwiatkowski, M., Abramjuk, C., Stephan, C., Haese, A., Chun, F., Schnorr, D., Loening, S. A., & Jung, K. (2005). A multicenter clinical trial on the use of (-5, -7) pro prostate specific antigen. *The Journal of Urology*, *174*, 2150–2153.
10. Catalona, W. J., Partin, A. W., Slawin, K. M., Brawer, M. K., Flanigan, R. C., Patel, A., Richie, J. P., deKernion, J. B., Walsh, P. C., Scardino, P. T., Lange, P. H., Subong, E. N., Parson, R. E., Gasior, G. H., Loveland, K. G., & Southwick, P. C. (1998). Use of the percentage of free prostate-specific antigen to enhance differentiation of prostate cancer from benign prostatic disease: A prospective multicenter clinical trial. *JAMA*, *279*, 1542–1547.
11. Steuber, T., O'Brien, M. F., & Lilja, H. (2008). Serum markers for prostate cancer: A rational approach to the literature. *European Urology*, *54*, 31–40.
12. Braun, K., Sjoberg, D. D., Vickers, A. J., Lilja, H., & Bjartell, A. S. (2016). A Four-kallikrein Panel Predicts High-grade Cancer on Biopsy: Independent Validation in a Community Cohort *European Urology*, *69*(3), 505511
13. Morote, J., Celma, A., Planas, J., Placer, J., Ferrer, R., de Torres, I., Pacciuci, R., & Olivan, M. (2016). Diagnostic accuracy of prostate health index to identify aggressive prostate cancer. An Institutional validation study. *Actas Urologicas Espanolas*, *40*, 378–385.
14. Gronberg, H., Adolfsson, J., Aly, M., Nordstrom, T., Wiklund, P., Brandberg, Y., Thompson, J., Wiklund, F., Lindberg, J., Clements, M., Egevad, L., & Eklund, M. (2015). Prostate cancer screening in men aged 50-69 years (STHLM3): A prospective population-based diagnostic study. *The Lancet Oncology*, *16*, 1667–1676.
15. Strom, P., Nordstrom, T., Aly, M., Egevad, L., Gronberg, H., & Eklund, M. (2018). The Stockholm-3 Model for prostate cancer detection: Algorithm update, biomarker contribution, and reflex test potential. *European Urology*, *74*, 204–210.
16. Ahmed, H. U., El-Shater Bosaily, A., Brown, L. C., Gabe, R., Kaplan, R., Parmar, M. K., Collaco-Moraes, Y., Ward, K., Hindley, R. G., Freeman, A., Kirkham, A. P., Oldroyd, R., Parker, C., & Emberton, M. (2017). Diagnostic accuracy of multi-parametric MRI and TRUS biopsy in prostate cancer (PROMIS): A paired validating confirmatory study. *Lancet*, *389*, 815–822.
17. Kasivisvanathan, V., Rannikko, A. S., Borghi, M., Panebianco, V., Mynderse, L. A., Vaarala, M. H., Briganti, A., Budäus, L., Hellawell, G., Hindley, R. G., Roobol, M. J., Eggener, S., Ghei, M., Villers, A., Bladou, F., Villeirs, G. M., Virdi, J., Boxler, S., Robert, G., & Moore, C. M. (2018). MRI-targeted or standard biopsy for prostate-cancer diagnosis. *New England Journal of Medicine*, *378*, 1767–1777.
18. Elwenspoek, M. M. C., Sheppard, A. L., McInnes, M. D. F., Merriel, S. W. D., Rowe, E. W. J., Bryant, R. J., Donovan, J. L., & Whiting, P. (2019). Comparison of multiparametric magnetic resonance imaging and targeted biopsy with systematic biopsy alone for the diagnosis of prostate cancer: A systematic review and meta-analysis. *JAMA Network Open*, *2*, e198427.
19. Bryant, R. J., Hobbs, C. P., Eyre, K. S., Davies, L. C., Sullivan, M. E., Shields, W., Sooriakumaran, P., Verrill, C. L., Gleeson, F. V., MacPherson, R. E., Hamdy, F. C., & Brewster, S. F. (2019). Comparison of Prostate Biopsy with or without Prebiopsy Multiparametric Magnetic Resonance Imaging for Prostate Cancer Detection: An Observational Cohort Study *The Journal of Urology*, *201*(3), 510519
20. Bryant, R. J., Yang, B., Philippou, Y., Lam, K., Obiakor, M., Ayers, J., Chiocchia, V., Gleeson, F., MacPherson, R., Verrill, C., Sooriakumaran, P., Hamdy, F. C., & Brewster, S. F. (2018). Does the introduction of prostate multiparametric magnetic resonance imaging into the active surveillance protocol for localized prostate cancer improve patient reclassification? *BJU International*, *122*, 794–800.
21. Carlsson, A., Wingren, C., Ingvarsson, J., Ellmark, P., Baldertorp, B., Ferno, M., Olsson, H., & Borrebaeck, C. A. (2008). Serum proteome

profiling of metastatic breast cancer using recombinant antibody microarrays. *European Journal of Cancer*, *44*, 472–480.
22. Pauly, F., Smedby, K. E., Jerkeman, M., Hjalgrim, H., Ohlsson, M., Rosenquist, R., Borrebaeck, C. A., & Wingren, C. (2014). Identification of B-cell lymphoma subsets by plasma protein profiling using recombinant antibody microarrays. *Leukemia Research*, *38*, 682–690.
23. Borrebaeck, C. A., Sturfelt, G., & Wingren, C. (2014). Recombinant antibody microarray for profiling the serum proteome of SLE. *Methods in Molecular Biology*, *1134*, 67–78.
24. Gerdtsson, A. S., Wingren, C., Persson, H., Delfani, P., Nordstrom, M., Ren, H., Wen, X., Ringdahl, U., Borrebaeck, C. A., & Hao, J. (2016). Plasma protein profiling in a stage defined pancreatic cancer cohort - Implications for early diagnosis. *Molecular Oncology*, *10*, 1305–1316.
25. Ingvarsson, J., Larsson, A., Sjoholm, A. G., Truedsson, L., Jansson, B., Borrebaeck, C. A., & Wingren, C. (2007). Design of recombinant antibody microarrays for serum protein profiling: Targeting of complement proteins. *Journal of Proteome Research*, *6*, 3527–3536.
26. Hamdy, F. C., Donovan, J. L., Lane, J. A., Mason, M., Metcalfe, C., Holding, P., Davis, M., Peters, T. J., Turner, E. L., Martin, R. M., Oxley, J., Robinson, M., Staffurth, J., Walsh, E., Bollina, P., Catto, J., Doble, A., Doherty, A., Gillatt, D., & Neal, D. E. (2016). 10-Year outcomes after monitoring, surgery, or radiotherapy for localized prostate cancer. *The New England Journal of Medicine*, *375*, 1415–1424.
27. Zegers, I., Keller, T., Schreiber, W., Sheldon, J., Albertini, R., Blirup-Jensen, S., Johnson, M., Trapmann, S., Emons, H., Merlini, G., & Schimmel, H. (2010). Characterization of the new serum protein reference material ERM-DA470k/IFCC: Value assignment by immunoassay. *Clinical Chemistry*, *56*, 1880–1888.
28. Soderlind, E., Strandberg, L., Jirholt, P., Kobayashi, N., Alexeiva, V., Aberg, A. M., Nilsson, A., Jansson, B., Ohlin, M., Wingren, C., Danielsson, L., Carlsson, R., & Borrebaeck, C. A. (2000). Recombining germline-derived CDR sequences for creating diverse single-framework antibody libraries. *Nature Biotechnology*, *18*, 852–856.
29. Sall, A., Walle, M., Wingren, C., Muller, S., Nyman, T., Vala, A., Ohlin, M., Borrebaeck, C. A. K., & Persson, H. (2016). Generation and analyses of human synthetic antibody libraries and their application for protein microarrays. *Protein Engineering, Design & Selection: PEDS*, *29*, 427–437.
30. Borrebaeck, C. A., & Wingren, C. (2011). Recombinant antibodies for the generation of antibody arrays. *Methods in Molecular Biology*, *785*, 247–262.
31. Pauly, F., Dexlin-Mellby, L., Ek, S., Ohlin, M., Olsson, N., Jirstrom, K., Dictor, M., Schoenmakers, S., Borrebaeck, C. A., & Wingren, C. (2013). Protein expression profiling of formalin-fixed paraffin-embedded tissue using recombinant antibody microarrays. *Journal of Proteome Research*, *12*, 5943–5953.
32. Kristensson, M., Olsson, K., Carlson, J., Wullt, B., Sturfelt, G., Borrebaeck, C. A., & Wingren, C. (2012). Design of recombinant antibody microarrays for urinary proteomics. *Proteomics Clinical Applications*, *6*, 291–296.
33. Gustavsson, E., Ek, S., Steen, J., Kristensson, M., Algenas, C., Uhlen, M., Wingren, C., Ottosson, J., Hober, S., & Borrebaeck, C. A. (2011). Surrogate antigens as targets for proteome-wide binder selection. *New Biotechnology*, *28*, 302–311.
34. Carlsson, A., Wuttge, D. M., Ingvarsson, J., Bengtsson, A. A., Sturfelt, G., Borrebaeck, C. A., & Wingren, C. (2011). Serum protein profiling of systemic lupus erythematosus and systemic sclerosis using recombinant antibody microarrays. *Molecular & Cellular Proteomics: MCP*, *10*, M110.005033.
35. Dexlin-Mellby, L., Sandstrom, A., Centlow, M., Nygren, S., Hansson, S. R., Borrebaeck, C. A., & Wingren, C. (2010). Tissue proteome profiling of preeclamptic placenta using recombinant antibody microarrays. *Proteomics Clinical Applications*, *4*, 794–807.
36. Ingvarsson, J., Wingren, C., Carlsson, A., Ellmark, P., Wahren, B., Engstrom, G., Harmenberg, U., Krogh, M., Peterson, C., & Borrebaeck, C. A. (2008). Detection of pancreatic cancer using antibody microarray-based serum protein profiling. *Proteomics*, *8*, 2211–2219.
37. Wingren, C., Ingvarsson, J., Dexlin, L., Szul, D., & Borrebaeck, C. A. (2007). Design of recombinant antibody microarrays for complex proteome analysis: Choice of sample labeling-tag and solid support. *Proteomics*, *7*, 3055–3065.
38. Kuhn, M. (2008). Building Predictive Models in R Using the caret Package *Journal of Statistical Software*, *28*(5), 126
39. Johnson W. Evan, Li Cheng, Rabinovic Ariel, Adjusting batch effects in microarray expression data using empirical Bayes methods *Biostatistics* 2007, *8*, (1), 118.127https://doi.org/10.1093/biostatistics/kxj037.
40. Carlsson, A., Wingren, C., Kristensson, M., Rose, C., Ferno, M., Olsson, H., Jernstrom, H., Ek, S., Gustavsson, E., Ingvar, C., Ohlsson, M., Peterson, C., & Borrebaeck, C. A. (2011). Molecular serum portraits in patients with primary breast cancer predict the development of distant metastases. *Proceedings of the National Academy of Sciences of the United States of America*, *108*, 14252–14257.
41. Kolde, R., Laur, S., Adler, P., & Vilo, J. (2012). Robust rank aggregation for gene list integration and meta-analysis. *Bioinformatics*, *28*, 573–580.
42. Damodaran, S., Kyriakopoulos, C. E., & Jarrard, D. F. (2017). Newly diagnosed metastatic prostate cancer: Has the paradigm changed? *The Urologic clinics of North America*, *44*, 611–621.
43. Smith, C. P., Laucis, A., Harmon, S., Mena, E., Lindenberg, L., Choyke, P. L., & Turkbey, B. (2019). Novel imaging in detection of metastatic prostate cancer. *Current Oncology Reports*, *21*, 31.
44. Sonn, G. A., Fan, R. E., Ghanouni, P., Wang, N. N., Brooks, J. D., Loening, A. M., Daniel, B. L., To'o, K. J., Thong, A. E., & Leppert, J. T. (2019). Prostate magnetic resonance imaging interpretation varies substantially across radiologists. *European Urology Focus*, *5*, 592–599.
45. Day, K. C., Lorenzatti Hiles, G., Kozminsky, M., Dawsey, S. J., Paul, A., Broses, L. J., Shah, R., Kunja, L. P., Hall, C., Palanisamy, N., Daignault-Newton, S., El-Sawy, L., Wilson, S. J., Chou, A., Ignatoski, K. W., Keller, E., Thomas, D., Nagrath, S., Morgan, T., & Day, M. L. (2017). HER2 and EGFR overexpression support metastatic progression of prostate cancer to bone. *Cancer Research*, *77*, 74–85.
46. Kharmate, G., Hosseini-Beheshti, E., Caradec, J., Chin, M. Y., & Tomlinson Guns, E. S. (2016). Epidermal growth factor receptor in prostate cancer derived exosomes. *Plos One*, *11*, e0154967.
47. Osman, I., Mikhail, M., Shuch, B., Clute, M., Cheli, C. D., Ghani, F., Thiel, R. P., & Taneja, S. S. (2005). Serum levels of shed Her2/neu protein in men with prostate cancer correlate with disease progression. *The Journal of Urology*, *174*, 2174–2177.
48. Lee, M. H., Jung, S.-Y., Kang, S. H., Song, E. J., Park, I. H., Kong, S.-Y., Kwon, Y. M., Lee, K. S., Kang, H.-S., & Lee, E. S. (2016). The significance of serum HER2 levels at diagnosis on intrinsic subtype-specific outcome of operable breast cancer patients. *Plos One*, *11*, e0163370.
49. Gaafar, R., Bahnassy, A., Abdelsalam, I., Kamel, M. M., Helal, A., Abdel-Hamid, A., Eldin, N. A., & Mokhtar, N. (2010). Tissue and serum EGFR as prognostic factors in malignant pleural mesothelioma. *Lung Cancer*, *70*, 43–50.
50. Lehrer, S., Diamond, E. J., Mamkine, B., Stone, N. N., & Stock, R. G. (2004). Serum interleukin-8 is elevated in men with prostate cancer and bone metastases. *Technology in Cancer Research & Treatment*, *3*, 411.
51. Maynard Janielle P., Ertunc Onur, Kulac Ibrahim, Baena-Del Valle Javier A., De Marzo Angelo M., Sfanos Karen S., IL8 Expression Is Associated with Prostate Cancer Aggressiveness and Androgen Receptor Loss in Primary and Metastatic Prostate Cancer *Molecular Cancer Research* 2020, *18*, (1), 153.165https://doi.org/10.1158/1541-7786.mcr-19-0595.
52. Kim, S. J., Uehara, H., Karashima, T., McCarty, M., Shih, N., & Fidler, I. J. (2001). Expression of interleukin-8 correlates with angiogenesis, tumorigenicity, and metastasis of human prostate cancer cells implanted orthotopically in nude mice. *Neoplasia*, *3*, 33–42.

53. Aalinkeel, R., Nair, M. P. N., Sufrin, G., Mahajan, S. D., Chadha, K. C., Chawda, R. P., & Schwartz, S. A. (2004). Gene expression of angiogenic factors correlates with metastatic potential of prostate cancer cells. *Cancer Research*, *64*, 5311–5321.
54. Li, X., Loberg, R., Liao, J., Ying, C., Snyder, L. A., Pienta, K. J., & McCauley, L. K. (2009). A destructive cascade mediated by CCL2 facilitates prostate cancer growth in bone. *Cancer Research*, *69*, 1685–1692.
55. Duque, J. L., Loughlin, K. R., Adam, R. M., Kantoff, P. W., Zurakowski, D., & Freeman, M. R. (1999). Plasma levels of vascular endothelial growth factor are increased in patients with metastatic prostate cancer. *Urology*, *54*, 523–527.
56. Goldstein, R., Hanley, C., Morris, J., Cahill, D., Chandra, A., Harper, P., Chowdhury, S., Maher, J., & Burbridge, S. (2011). Clinical investigation of the role of interleukin-4 and interleukin-13 in the evolution of prostate cancer. *Cancers*, *3*, 4281–4293.
57. Comperat, E., Roupret, M., Drouin, S. J., Camparo, P., Bitker, M. O., Houlgatte, A., Cancel-Tassin, G., & Cussenot, O. (2010). Tissue expression of IL16 in prostate cancer and its association with recurrence after radical prostatectomy. *The Prostate*, *70*, 1622–1627.
58. Nakashima, J., Tachibana, M., Horiguchi, Y., Oya, M., Ohigashi, T., Asakura, H., & Murai, M. (2000). Serum interleukin 6 as a prognostic factor in patients with prostate cancer. *Clinical Cancer Research: An Official Journal of the American Association for Cancer Research*, *6*, 2702–2706.
59. Rojas, A., Liu, G., Coleman, I., Nelson, P. S., Zhang, M., Dash, R., Fisher, P. B., Plymate, S. R., & Wu, J. D. (2011). IL-6 promotes prostate tumorigenesis and progression through autocrine cross-activation of IGF-IR. *Oncogene*, *30*, 2345–2355.
60. Vaday, G. G., Peehl, D. M., Kadam, P. A., & Lawrence, D. M. (2006). Expression of CCL5 (RANTES) and CCR5 in prostate cancer. *The Prostate*, *66*, 124–134.
61. Inoue, K., Slaton, J. W., Eve, B. Y., Kim, S. J., Perrotte, P., Balbay, M. D., Yano, S., Bar-Eli, M., Radinsky, R., Pettaway, C. A., & Dinney, C. P. N. (2000). Interleukin 8 expression regulates tumorigenicity and metastases in androgen-independent prostate cancer. *Clinical Cancer Research*, *6*, 2104–2119.
62. Kim, S. J., Uehara, H., Karashima, T., McCarty, M., Shih, N., & Fidler, I. J. (2001). Expression of interleukin-8 correlates with angiogenesis, tumorigenicity, and metastasis of human prostate cancer cells implanted orthotopically in nude mice. *Neoplasia*, *3*, 33–42.
63. Lee, S. O., Lou, W., Hou, M., de Miguel, F., Gerber, L., & Gao, A. C. (2003). Interleukin-6 promotes androgen-independent growth in LNCaP human prostate cancer cells. *Clinical Cancer Research: An Official Journal of the American Association for Cancer Research*, *9*, 370–376.

SUPPORTING INFORMATION

Additional supporting information may be found online https://doi.org/10.1002/prca.202000025 in the Supporting Information section at the end of the article.

How to cite this article: Emruli, V. K., Liljedahl, L., Axelsson, U., et al. (2021). Identification of a serum biomarker signature associated with metastatic prostate cancer. *Proteomics Clinical Applications*, e2000025. https://doi.org/10.1002/prca.202000025